Genetics in Medicine

ARTICLE

Biallelic variants in *CRIPT* cause a Rothmund-Thomson-like syndrome with increased cellular senescence

ABSTRACT

Purpose: Rothmund-Thomson syndrome (RTS) is characterized by poikiloderma, sparse hair, small stature, skeletal defects, cancer, and cataracts, resembling features of premature aging. *RECQL4* and *ANAPC1* are the 2 known disease genes associated with RTS in >70% of cases. We describe RTS-like features in 5 individuals with biallelic variants in *CRIPT* (OMIM 615789).
Methods: Two newly identified and 4 published individuals with *CRIPT* variants were systematically compared with those with RTS using clinical data, computational analysis of photographs, histologic analysis of skin, and cellular studies on fibroblasts.
Results: All *CRIPT* individuals fulfilled the diagnostic criteria for RTS and additionally had neurodevelopmental delay and seizures. Using computational gestalt analysis, *CRIPT* individuals showed greatest facial similarity with individuals with RTS. Skin biopsies revealed a high expression of senescence markers (p53/p16/p21) and the senescence-associated ß-galactosidase activity was elevated in CRIPT-deficient fibroblasts. RECQL4- and CRIPT-deficient fibroblasts showed an unremarkable mitotic progression and unremarkable number of mitotic errors and no or only mild sensitivity to genotoxic stress by ionizing radiation, mitomycin C, hydroxyurea, etoposide, and potassium bromate.
Conclusion: *CRIPT* causes an RTS-like syndrome associated with neurodevelopmental delay and epilepsy. At the cellular level, RECQL4- and CRIPT-deficient cells display increased senescence, suggesting shared molecular mechanisms leading to the clinical phenotypes.
© 2023 by American College of Medical Genetics and Genomics. Published by Elsevier Inc.

Introduction

Rothmund-Thomson syndrome (RTS) is a rare autosomal recessive disorder, which is characterized by clinical signs of premature aging and increased risk of cancer. The classical skin presentation is poikiloderma consisting of chronic, reticulated areas of depigmentation and hyperpigmentation, dilated blood vessels, and punctate atrophy giving a mottled appearance.[1] Additional features of RTS include sparse hair, dystrophic teeth and nails, short stature, skeletal abnormalities including osteopenia, and juvenile cataracts.[2]

More than 300 individuals with RTS have been reported in the literature since its first description in 1868.[3,4] Two forms of RTS can be distinguished. The characteristic feature of RTS type 1 is cataracts, and the typical hallmark of RTS type 2 is an increased susceptibility to cancer,

*Correspondence and requests for materials should be addressed to Luisa Averdunk, Department of General Pediatrics, Neonatology and Pediatric Cardiology, University Children's Hospital, Heinrich-Heine-University, Moorenstraße 5, 40225 Düsseldorf, Germany. *Email address:* luisasusan.averdunk@med.uni-duesseldorf.de OR Felix Distelmaier, Department of General Pediatrics, Neonatology and Pediatric Cardiology, University Children's Hospital, Heinrich-Heine-University, Moorenstraße 5, 40225 Düsseldorf, Germany. *Email address:* felix.distelmaier@med.uni-duesseldorf.de
A full list of authors and affiliations appears at the end of the paper.

Key Messages

1. *CRIPT* causes a Rothmund-Thomson-like syndrome, which is associated with developmental delay.
2. Biallelic variants in *CRIPT* cause increased cellular senescence, which is a shared cellular phenotype of CRIPT and RECQL4 deficiencies.
3. In fibroblasts derived from individuals with pathogenic variants in *CRIPT*, mitotic progression and mitotic arrest induction are not compromised, and the incidence of mitotic errors is not significantly increased.
4. Fibroblasts from *CRIPT* and *RECQL4* individuals show no or only very mild sensitivity to ionizing radiation, mitomycin C, hydroxyurea, etoposide, and potassium bromate compared with controls.

particularly osteosarcoma.[2] Neurodevelopmental delay of variable degree has been reported in RTS, but it has not been formally studied.[5-9] The diagnosis of RTS can be made on clinical grounds based on the characteristic poikiloderma and other typical features of RTS (small stature, osteosarcoma or skin cancer, cataracts, and sparse hair).[2] Numerical and structural chromosomal aberrations have been observed in lymphocytes and fibroblasts from RTS individuals.[2,10,11]

In 1999, biallelic variants in *RECQL4* were identified in a subset of RTS type 2 cases.[12] Although the genetic cause of RTS type 1 remained unknown for a long time, biallelic variants in *ANAPC1*, including intronic splice variants, were recently identified explaining a proportion of RTS type 1.[13] *RECQL4* codes for the ATP-dependent RECQ-like DNA helicase type 4 (RECQL4) and is involved in DNA repair, DNA replication, telomeric maintenance, normal chromosome alignment in mitosis, and senescence.[14-18] RECQL4 contains a conserved DNA-unwinding domain, but it has only weak helicase activity.[19] *ANAPC1* codes for the APC1 subunit of the multisubunit anaphase-promoting complex or cyclosome (APC/C). APC/C is an E3 ubiquitin ligase that controls cell cycle progression by proteasome-dependent degradation of cell cycle regulators.[20] The genetic cause in approximately 30% of RTS cases remains unknown, suggesting that not all RTS-associated genes have been identified so far.[21]

We report 2 unrelated individuals who fulfilled the diagnostic criteria of RTS but lacked pathogenic variants in *RECQL4* and *ANAPC1*. However, we identified pathogenic biallelic variants in *CRIPT* by exome sequencing. Biallelic variants in *CRIPT* were recently associated with primordial dwarfism and developmental delay in 4 families, but a link to RTS has not been drawn so far.[22-24] *CRIPT* codes for a short, 101 amino acid cysteine-rich PDZ-binding protein that specifically binds to microtubules and to the **p**ost synaptic density protein, **d**rosophila disc large tumor suppressor and **z**onula occludens-1-(PDZ) domain 3 of the postsynaptic density protein 95 (PDS95). CRIPT has mainly been studied

in the context of synaptic formation; however, a functional role for CRIPT outside of the brain is unknown.[25,26] Here, we systematically compare *CRIPT*-associated clinical phenotypes with RTS and identify *CRIPT* as a novel disease gene associated with an RTS-like phenotype. To delineate the driving and shared molecular mechanisms underlying RTS, cellular senescence, mitotic progression, and DNA repair were studied in fibroblasts from RECQL4- and CRIPT-deficient individuals. We show that *CRIPT* and *RECQL4* both play a functional role in preventing cellular senescence, whereas the mechanism that drives senescence remains unsolved.

Materials and Methods

Patient recruitment and clinical evaluation

Two individuals with typical features of RTS (#1 and #2) underwent exome sequencing. From the 3 individuals (#3-5) with biallelic *CRIPT* variants (*CRIPT* individuals) from the literature, follow-up clinical data and updated photographs were provided.[22,23] Skin biopsies of #1 and #3 were performed and used for cell culture of fibroblasts and immunohistochemistry. Similarities among facial photographs were quantified using GestaltMatcher.[27] Frontal photographs from the 5 *CRIPT* individuals were compared with available, open-access photographs of published RTS cases (*RECQL4*), RecQ family–related syndromes, and syndromes characterized by poikiloderma. References of photographs are accessible in GestaltMatcher Database (https://db.gestaltmatcher.org). Methods of exome sequencing, electron microscopy of hair, and diagnostic skin histology are provided in the Supplemental Methods.

Experimental methods

Fresh skin biopsies for the generation of fibroblasts cultures were available from *CRIPT* individuals #1, #2, and #3, and from control individuals (infants and adolescents).[28] The fibroblasts of #3 divided very slowly, and the number of cells was sufficient for live-cell imaging of mitotic progression but not for assays of senescence or genome stability. Fibroblasts from RTS individuals with pathogenic variants in *RECQL4* (*RECQL4* individuals) were obtained from Coriell Institute (NJ): *RECQL4* #1, AG05013: NM_004260.4:c.2492_2493del p.(His831Argfs*52), NM_004260.4:c.2059-1G>T, compound heterozygous; *RECQL4* #2, AG18371: NM_004260.4:c.1483+27_1483+37del, homozygous; and *RECQL4* #3, AG17524A: NM_004260.4:c.1391-1G>A NM_004260.4:c.2492_2493del p.(His831Argfs*52), compound heterozygous. The neonatal control fibroblast line was obtained from Lonza (Walkersville). The other control fibroblasts were generated by skin biopsies from healthy individuals. Fibroblasts with pathogenic variants in *ANAPC1* were not available. Cellular ß-galactosidase activity was quantified in fibroblasts

from #1 and #2 and after downregulation of CRIPT expression by small interfering RNA (siRNA) in control cells using the CellEvent Senescence Green Flow Cytometry Kit (Thermo Fisher). Lymphocytes from whole blood samples of #1 were analyzed by optical genome mapping to search for somatic structural variants (Bionano Genomics). Mitotic progression of fibroblasts was analyzed after DNA staining in a Ti2 Eclipse (Nikon) equipped with an LED light engine SpectraX (Lumecor, Beaverton) and a Plan-Apochromat 20× NA 0.75 objective and environmental control system UNO-T-H-CO2 (Okölab). Fluorescence multiposition imaging was done every 3 minutes for 24 hours using the Elements software (Nikon). The dwell times and the images of mitotic progression were extracted using the machine learning CecogAnalyzer 1.5.2.[29] Mitotic arrest was induced with 100 ng/mL nocodazole treatment for 30 minutes. To study the sensitivity of patient-derived cell lines to genotoxic stress, cell viability was quantified at high resolution and high sensitivity using IncuCyte-S3 Live-Cell-Imaging system (Essen Bioscience). After treatment of cells with different genotoxic agents, viable and dead cells were stained and tracked for 96 hours. A cell death score was calculated as the dead cell over live-cell signal, allowing for normalization of different growth kinetics. Comprehensive description of methods, including siRNA downregulation, optical mapping, cytoplasmic and nuclear extraction of CRIPT protein, and mitotic progression are provided in the Supplemental Methods.

Statistical analysis

Differences of ß-galactosidase activity was compared using student's *t*-test, and live-cell imaging-based mitotic timing and cell viability was analyzed with one-way analysis of variance.

Results

Clinical characteristics

Individual #1 is a 3-year-old Moroccan female born in Germany who presented at the age of 6 months with a cutaneous rash starting on the face and spreading to the hands and legs, sparing the trunk, and developing into reticulated hypo- and hyperpigmentation with punctate atrophy resembling poikiloderma (Figure 1B).

Individual #2 is an 8-year-old Romanian male born in Northern Ireland by cesarean delivery at 28 weeks of gestation because of intrauterine growth retardation. Starting at 4 weeks of age, he had a mottled, reticulated rash affecting the limbs and abdomen spreading to the hands and scalp. In both individuals, edematous swelling of the limbs and palmoplantar hyperkeratotic lesions accompanied the skin rash. Histologic examination of skin biopsies from both individuals revealed atrophic epidermis, inflammatory

infiltration, pigment incontinence, and dilated blood vessels confirming the diagnosis poikiloderma (Figure 1F).[1] Additional histologic findings were fragmented elastic fibers and increased mucinous deposits (Supplemental Figure 1).

Both individuals had sparse hair, including eyebrows and eyelashes (Figure 1B and C). The children showed failure to thrive (Figure 1G), and full skeletal survey indicated osteopenia and skeletal abnormalities (Figure 1H). Individual #2 was diagnosed with bilateral central cataract at the age of 8 years. Both children had muscular hypotonia and moderate motor and profound language delay. Head magnetic resonance imaging showed reduced brain volume. Individual #2 had microcephaly (Figure 1I). Both had a prominent forehead with frontal bossing, a broad, depressed nasal root, and telecanthal folds.

In summary, the clinical features included poikiloderma, sparse hair, short stature, skeletal anomalies, developmental delay, and facial dysmorphic features. Because the diagnostic criteria of RTS were fulfilled, RTS was diagnosed on clinical grounds (Table 1).[2]

Identification of homozygous variants in *CRIPT* in 2 individuals with RTS

There were no pathogenic variants in *RECQL4* or *ANAPC1* identified by exome sequencing, and protein expression of APC1 and RECQL4 was normal in fibroblasts from individuals #1 and #2 (Figure 2B). By Sanger sequencing of individual #1, we additionally did not detect the recurrent deep intronic c.2705−198C>T variant that had been identified in *ANAPC1* (Supplemental Figure 2A).[13]

Instead, in both individuals, we identified homozygous variants in the *CRIPT* gene (Figure 1J). In 4 families (#3-6), pathogenic *CRIPT* variants were reported in association with abnormal skeletal and neurologic development and abnormal skin (Table 1).[22-24] The term "short stature with microcephaly and distinctive facies" was suggested (OMIM 615789).[22,23]

Individual #1 harbors the homozygous variant c.132del (NM_014171.4), which results in the same frameshift p.(Ala45Glnfs*86) that has been reported in individual #3 (ACMG class 5).[23] The missense variant c.227G>A, p.(Cys76Tyr) (NM_014171.4) of #2 is unreported (highly conserved among different species, including mammals, zebrafish, chicken, frog, and African craw frog; Combined Annotation Dependent Depletion score 31, https://cadd.gs.washington.edu/). The variant reported by Leduc et al[22] (#5) also is a missense variant substituting one of the 8 cysteine residues in 101-aa CRIPT (Figure 1J). The cysteine residues have recently been suggested to play a crucial role in redox modulation during disassembly of mitotic spindle.[22,30] The variants have been confirmed by Sanger sequencing in the probands' parents (Supplemental Figure 2B). By western blot of CRIPT protein in patient-derived fibroblast cell lysates, CRIPT was only detectable in control and RECQL4 individuals but not in CRIPT
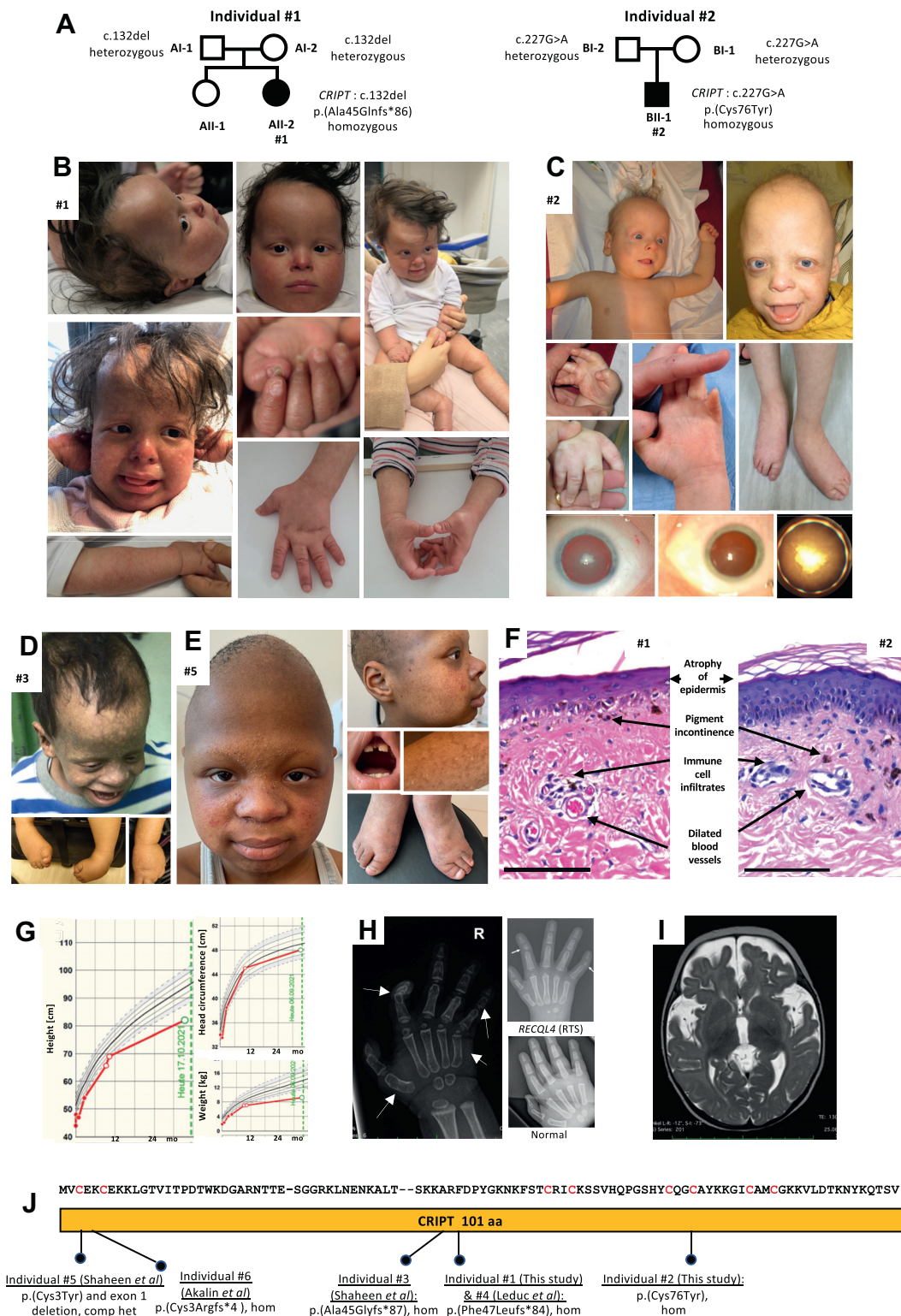
Figure 1   **Genetic, clinical and imaging findings in individuals with biallelic variants in *CRIPT*.** A. Family pedigrees of the *CRIPT* individual #1 (Moroccan) and #2 (Romanian) both harboring homozygous pathogenic variants in *CRIPT* (NM_014171.4.). B. Photographs of individual #1 showing characteristic frontal bossing, depressed nasal root, telecanthus, reticulated pigmentation of the skin (1 year), progressive hair loss with absent eye lashes and eyebrows, edematous swelling of extremities, muscular hypotonia, and dystrophic nails. Proximal placed and short thumbs. Difficulties to grasp with thumb and finger (first row: 1 year, second row: 2 years, hands: 4 years). C. Photographs of individual #2 showing sparse hair and progressive hair loss, reticulated rash of cheeks, dystrophic nails, and proximally placed thumb and edematous swelling, talipes equinus and nuclear cataract of both eyes (cataract of left eye only visible under the operating microscope). D, E. Photographs of individuals #3 and #5 at their follow-up examinations (unpublished photos of published cases)[22,23] #3 at

individuals (Figure 3B). Despite the clinical features resembling RTS in our subjects, a link between *CRIPT* and RTS has not been previously established.

Clinical comparison of *CRIPT* individuals with RTS

Clinical updates on *CRIPT* individuals #3-5 were obtained, and clinical features of RTS types 1 and 2 were systematically compared with the 6 *CRIPT* individuals (Table 1).[22-24] Individual #4 had died at the age of 70 days because of pulmonary infection. All *CRIPT* individuals who survived presented with reticulated, hypopigmented skin changes (5 of 5) compatible with poikiloderma, the hallmark of RTS (Figure 1B-E). All individuals had sparse hair and progressive hair loss, resulting in an almost complete absence of eyebrows and eyelashes in #1 and #2 (6 of 6). Additional features were dysplastic nails (2 of 5, #1 and #5) and delayed eruption of abnormal teeth (3 of 5, #1, #2, #5, and #6).[1] All *CRIPT* individuals had short stature (6 of 6). RTS often presents with skeletal anomalies, including osteoporosis, abnormal metaphyseal trabeculation, brachymesophalangy, first metacarpal or thumb hypoplasia, or hypoplastic terminal phalanges.[31] Skeletal survey of *CRIPT* individuals revealed osteopenia with abnormal metaphyseal striation (6 of 6), brachymesophalangy (3 of 6), first metacarpal hypoplasia (1 of 6), hypoplastic terminal phalanges (5 of 6), flexible talipes equinus or pes planus (6 of 6), and scoliosis (6 of 6). The typical feature distinguishing RTS type 1 from RTS type 2 are juvenile-onset cataracts.[13] Individual #2 developed bilateral cataracts at the age of 8 years, consistent with RTS type 1 individuals. Of 6 *CRIPT* individuals, 5 had myopia and 4 of 6 were suspected to have optic atrophy. RTS type 2 is associated with an increased risk of neoplasm, but none of the *CRIPT* individuals had a history of cancer so far.[2] Although RTS has rarely been associated with reduced brain volume or microcephaly, most RTS individuals are reported to develop normally or to only have mild speech delay.[5-7] All *CRIPT* individuals presented with moderate motor delay and clearly impaired language development (Supplemental Table 1: skills and development of #1 and #2). The oldest individual #5 was able to speak short sentences and read 3 to 4 letter words at the age of 11 years. All *CRIPT* individuals had proportionate microcephaly (5 of 6) or reduced brain volumes on magnetic resonance imaging (Figure 1J). Although epilepsy is not common in RTS, 4 of 6 *CRIPT* individuals developed epilepsy (difficult to control in #1 and 2; Supplemental Table 2). Of 5 individuals, 2 had postprandial

emesis and dysphagia improving with age. All individuals were affected by recurrent upper respiratory tract infections, and in RTS, recurrent infections have been reported although rare.[32] A laboratory workup of immunodeficiency revealed only mildly reduced titer of IgG in *CRIPT* individual #1. Additional hematologic findings included anisopoikilocytosis (2 of 6), microcytic anemia (2 of 6), and thrombocytopenia (1 of 6). RTS clinically overlaps with progeroid syndromes, including the 2 RecQ family–related syndromes (Bloom syndrome and Werner syndrome) and poikiloderma-associated syndromes (eg, Kindler syndrome and Fanconi anemia). We systematically compared the *CRIPT* individuals and RTS syndrome with these differential diagnoses, but none of the *CRIPT* individuals were more appropriately classified as any of these differential diagnoses than as RTS (Supplemental Table 3).[1] All *CRIPT* individuals fulfilled RTS diagnostic criteria and were additionally affected by neurodevelopmental delay, seizures, and microcephaly.

Sanger sequencing of *CRIPT* in 10 *RECQL4*-negative RTS individuals from the RTS registry

We searched for pathogenic variants in *CRIPT* in all ($N = 10$) *RECQL4*-negative RTS type 1 individuals from the RTS registry (Baylor College of Medicine, Houston, TX). Four of these individuals had mild developmental delay, and 6 had reportedly unremarkable neurologic development. Pathogenic variants in *CRIPT* were not detected in either of these 2 groups of individuals, which supports the notion that *CRIPT* is not a common disease gene among RTS individuals with unremarkable neurologic development.

Loss of cuticle in hair from *CRIPT* and *RECQL4* individuals

RECQL4 and *CRIPT* individuals have brittle and sparse hair. The healthy hair surface consists of several layers of overlapping cells, termed cuticle. Electron microscopy of the hair surface of *CRIPT* individuals revealed a partial (#2) to complete (#1) loss of the cuticle that was similar to that of the hair from 2 *RECQL4* individuals #1 and #2 (Figure 2A). Besides, the hair from #1 and #2 and *RECQL4 #1* showed fragility of the hair surface after bending stress. In contrast, the hair surface from young and old healthy controls showed intact cuticle layers.

---

the age of 11 years with reticulated hypo- and hyperpigmentation and sparse hair, edematous swelling, and talipes equinus, and #5 at the age of 10.5 years with reticulated rash on the cheeks, vesicles and hypo- and hyperpigmentation, and talipes equinus. F. Skin of #1 showing typical histopathologic findings of poikiloderma (H&E, 20×). Scale bars = 50 μm. G. Growth charts illustrating failure to thrive and short stature (dashed line illustrates third and 97th percentiles) of #1. H. Radiographic images of the hand of individual #1 showing osteopenia, brachymesophalangy third to fifth digits, metacarpal hypoplasia first and fifth and bowing of second and fifth digits (top middle panel), and hypoplastic terminal phalanges, in comparison to x-ray images of unaffected (bottom middle panel) and *RECQL4*/RTS (right panel) individuals[31] and a healthy control individual. I. MRI of the head showing reduced brain volume in *CRIPT* individual #1. J. Schematic illustration of CRIPT, a cysteine-rich PDZ domain-binding protein (cysteines in red). Pathogenic variants indicated. *MRI*, magnetic resonance imaging; *RTS*, Rothmund-Thomson syndrome.

Table 1 Clinical characteristics of *ANAPC1*, *RECQL4*, and *CRIPT* individuals

Feature	RTS Type 1	RTS Type 2	Individual #1 (New)	Individual #2 (New)	Individual #3 (Shaheen et al[23])	Individual #4 (Shaheen et al[23])	Individual #5 (Leduc et al[22])	Individual #6 (Akalin et al[24])
		RTS						
Disease gene	*ANAPC1*	*RECQL4*	*CRIPT*	*CRIPT*	*CRIPT*	*CRIPT*	*CRIPT*	*CRIPT*
Variants			c.132del p.(Ala45Glyfs*82), homozygous	c.227G>A, p.(Cys76Tyr), homozygous	c.133_134insGG, p.(Ala45Glyfs*82), homozygous	c.141del p.(Phe47Leufs*84), homozygous	c.8G>A p.(Cys3Tyr), 1,331 bp del exon 1, compound-heterozygous	c.7_8del; p.(Cys3Argfs*4), homozygous
Origin, sex			Morocco, female	Romania, male	Saudi Arabia, male	Saudi Arabia, male	African American, female	Turkey, male
Age at last follow-up			4 y	8 y	11 y	70 d	10.5 y	4 y
RTS—major criteria								
Facial rash	+	+	+	+	+	n/r	+	+
Poikiloderma	+	+	+	+	+	n/r	+	n/r
RTS—minor criteria (at least 2)								
Sparse hair	+	+	+	+	n/r	+ (silvery)	+	+
Short stature	+	+	+	+	+	+	+	+, reduced subcutaneous tissue
Neoplasia	−	+	−[a]	−[a]	−[a]	−[a]	−1	−1
Cataracts	+	−	−	+	−	−	−	−
Other clinical features								
Skeletal anomalies[78,79]								
Osteopenia/metaphyseal striations	+	−	+	+	+ (−1.8 z)	+	+	+
Brachydactyly/Brachymeso-phalangy	II + V	n/r	+ III + IV + V	n/r	+	n/r	+ (slender)	n/r
Metacarpal hypoplasia	I	n/r	I + V (plus mild bowing)	n/r	n/r	n/r	n/r	Delayed carpal ossification
Hypoplastic terminal phalanges	+	n/r	+ (no nail spikes)	+	+	+	+	n/r
Feet anomalies	−	−	Skewfoot	Pes planus	Pes planus	Skewfoot	Pes planus	Pes calcaneovalgus
Syndactyly of toes 4/5	−	−	+	+	+	+	+	+
Trunk anomalies			Scoliosis	Scoliosis + platyspondyly	Scoliosis + platyspondyly	Scoliosis 11 pairs of ribs	Scoliosis 11 pairs of ribs	Scoliosis
Aplastic radius, ulna, thumb	Common	−	Proximally placed thumb	−	−	−	−	−
Frontal bossing	+	+	+	+	+	+	+	+ and obliteration of metopic and sagittal sutures
Dystrophic nails	+	+	+	−	n/r	n/r	+	n/r
Abnormal teeth			+	+	n/r	n/r	+	+ (conic, delayed)
Microcephaly	Occasionally		−	+	+	+	+	+
Developmental delay	10%	10%	+	+	+	+	+	+

(continued)

Table 1 Continued

Feature	RTS Type 1	RTS Type 2	Individual #1 (New)	Individual #2 (New)	Individual #3 (Shaheen et al[23])	Individual #4 (Shaheen et al[23])	Individual #5 (Leduc et al[22])	Individual #6 (Akalin et al[24])
		RTS						
Motor development	Usually normal		Independent sitting at 15 mo, walking at 30 mo	Independent sitting at 12 mo, walking at 36 mo	Can run and jump, not able to ride bicycle	−	Independent sitting at 13 mo, walking at 23 mo	Independent sitting 30 mo, walking 4 y
Speech development	Mild delay		Single words, no sentences, understands simple commands	Single words, no sentences, understands simple commands	Single words, no sentences, understands simple commands	−	Speaks in short sentences, follows simple commands, reads 3-and 4-letter words	Significant delay
Gastrointestinal disturbance	Some		+ (dysphagia)	−	+ (mild dysphagia)	−	−	−
Recurrent chest infections	Rarely Recurrent (Kubota et al[32])		Yes	Yes	Yes	Yes, lethal pneumonia	Yes	Yes, hospitalized twice
Anemia			Macrocytic	n/r	n/r	Anisopoikilocytosis	Aniso-poikilocytosis	Yes, additionally thrombo-cytopenia
Additional features primarily in *CRIPT* individuals								
Seizures (age of onset)	−	−	+ (1 y) Well controlled	+ (3 y) Control difficult	−	+ (2 mo)	+ (3 y) Well controlled	−
Myopia	−	−	+	+	+	−	+	+
Retina	−	−	Normal	Normal	Bilateral optic atrophy macular dystrophy	Bilateral pale optic discs	Hypopigmented mottling retina	Retinal pigmentation defect

[a]No history of cancer at last follow-up.
Variants refer to the transcript NM_014171.4 (*CRIPT*).
+, present; −, not present; *n/r*, not reported; *RTS*, Rothmund-Thomson syndrome.
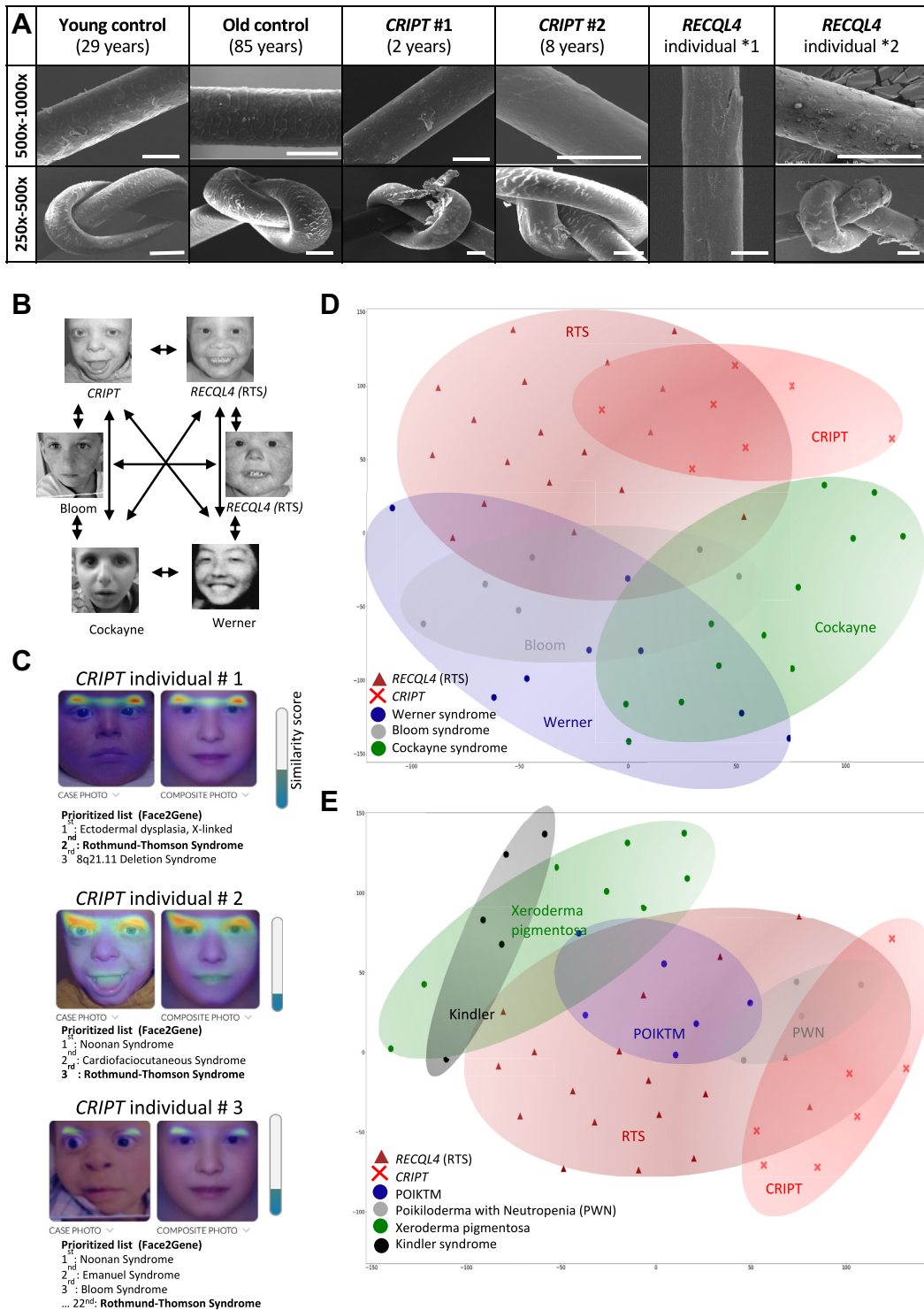
Figure 2   Comparison of hair ultrastructure and facial profile of individuals with CRIPT deficiency and differential diagnoses.
A. Electron microscopy showing the normal hair cuticle (overlapping layers of dead cells forming the hair surface) from young (29 years) and old (85 years) healthy controls (left panels) in comparison with (complete #1 or partial #2) loss of the cuticle in the hair from *CRIPT* and *RECQL4* individuals. Easy breaking of the hair shaft or surface after bending stress (knots). Scale bars = 50 μm. B. Illustration of pairwise computational comparison of facial morphology using the DeepGestalt analysis framework (Face2Gene, FDNA Inc)[33] C. Heatmaps of frontal images of *CRIPT* #1, #2, and #3 highlighting the facial regions (left side) with greatest overlaps with the merged, composite image RTS (*RECQL4*) individuals (right side) with prioritized lists of differential diagnoses based on the analysis of frontal images for *CRIPT* #1, #2, and #3. D. Analysis of the morphologic similarities of published photographs using GestaltMatcher. The 2D visualization illustrates the morphologic distances between facial images of *CRIPT* individuals, and individuals with pathogenic variants in *RECQL4* (RTS) and related syndromes—RecQ family–related syndromes (Bloom syndrome and Werner syndrome), and the progeroid Cockayne syndrome. E. The 2D visualization illustrates the morphologic distance of *CRIPT* and *RECQL4* individuals and other syndromes that are characterized by poikiloderma. *POIKTM*, hereditary fibrosing poikiloderma with tendon contractures, myopathy, and pulmonary fibrosis; *PWN*, poikiloderma with neutropenia; *RTS*, Rothmund-Thomson syndrome.
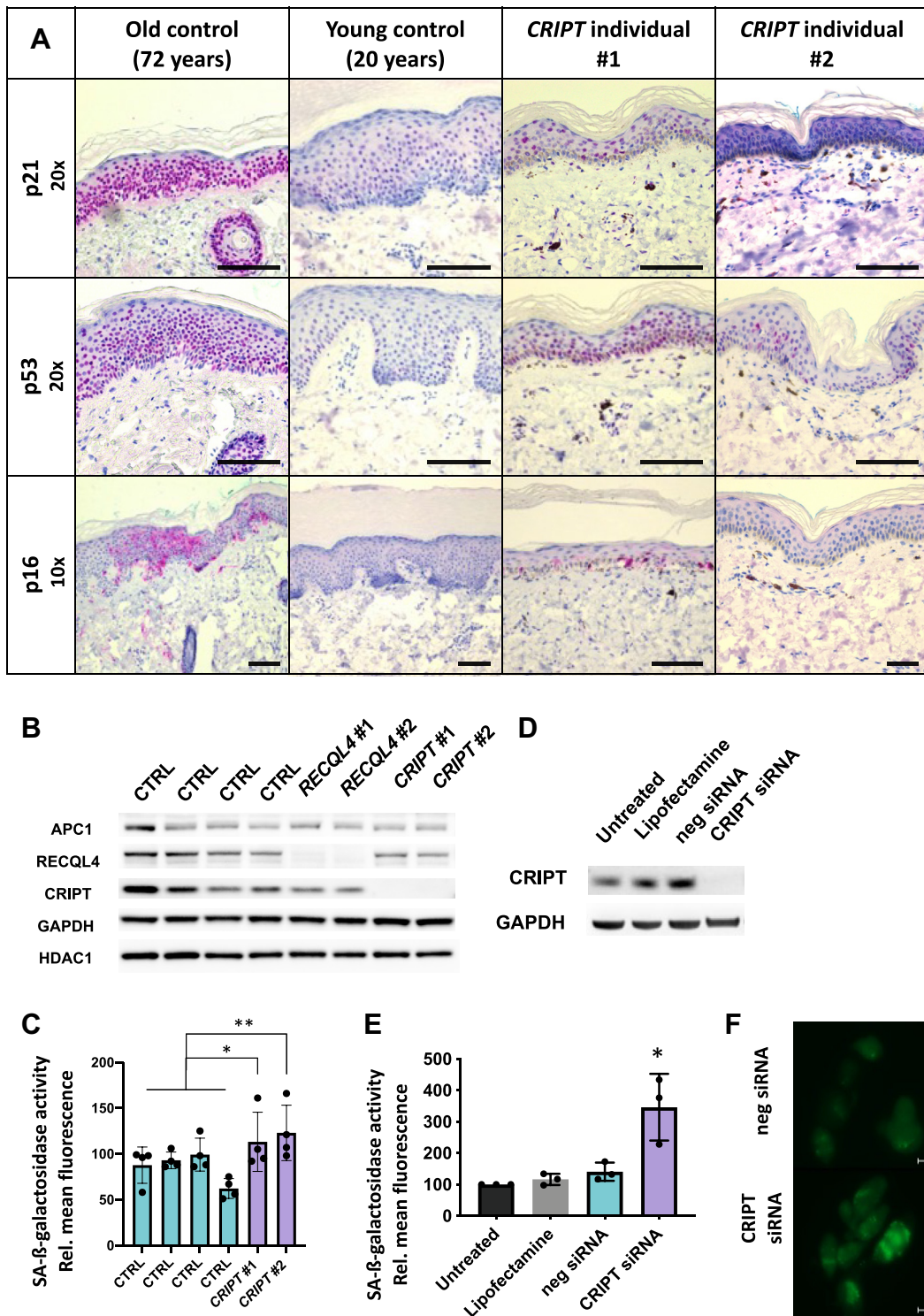
Figure 3 **Senescence markers in skin biopsies from CRIPT-deficient individuals and in CRIPT-deficient cultured fibroblasts.** A. Immunohistochemical staining of p21, p53, and p16 (senescence markers). Expression of the p21, p53, and p16 in the skin of a 72-year-old control individual and *CRIPT* individual #1, and expression of p53 and minor expression of p21 in *CRIPT* individual #2, but not in the 20-year-old individual. Scale bars = 50 μm. B. Western blot of APC1, RECQL4, and CRIPT from fibroblast cell lysates of *CRIPT* individuals #1 and #2 and RECQL4 cell lines #1 and #2. HDAC1 was used as a loading control for nuclear proteins. C. Senescence-associated-(SA-) ß-galactosidase activity in fibroblasts from controls and from *CRIPT* individuals #1 + #2. D. Immunoblotting of CRIPT after small interfering RNAmediated CRIPT downregulation in control fibroblasts. E, F. SA-ß-galactosidase activity in fibroblasts after downregulation of CRIPT expression on day 14. Scale bars = 10 μm. All experiments were performed 3 times. Mean ± SD. *APC1*, anaphase-promoting complex subunit 1; *CTRL*, control; *GAPDH*, glyceraldehyde 3-phosphate dehydrogenase; *HDAC1*, Hda1 histone deacetylase complex. * $P < .05$; ** $P < .01$.

Computational comparison of photographs

RTS is characterized by a distinct facial phenotype, which includes frontal bossing, depressed nasal root, and epicanthal folds.[1] All *CRIPT* individuals show these craniofacial features. However, the assessment of facial features is biased by the clinician's experience. Therefore, the facial appearance of *CRIPT* individuals ranging from #1 to #5 was compared with individuals with other syndromic genetic diagnoses using the unbiased, computational DeepGestalt analysis (Face2Gene and FDNA) (Figure 2B).[33] Based on photographs of #1 and #2, RTS was listed among the top 3 differential diagnoses, indicating a significant morphologic similarity (Figure 2C). For the photograph of #3 and #6, RTS was ranked as top 22 and top 9, respectively; for #4 and #5, RTS was not in the prioritized list of differential diagnoses, which might be attributed to a reduced performance of DeepGestalt for very young age or African background.

The morphologic similarity between *CRIPT* and *RECQL4* individuals and related differential diagnoses was quantified by GestaltMatcher.[27] The photographs of *CRIPT* individuals showed a strong overlap with *RECQL4* individuals but no overlap with the RecQ family–related Bloom, Werner, or Cockayne syndromes (Figure 2D)

Facial photographs of *CRIPT* individuals showed the highest similarity to images of *RECQL4* individuals when compared with other "poikiloderma syndromes" (Figure 2E). Interestingly, photographs of *RECQL4* and *CRIPT* individuals overlapped with hereditary fibrosing poikiloderma (POIKTM) with tendon contractures, myopathy, and pulmonary fibrosis and poikiloderma with neutropenia syndrome.

Increased senescence in skin and in CRIPT-deficient fibroblasts

CRIPT individuals display the typical hallmarks of aging. Aged tissues accumulate senescent cells with a permanently arrested cell cycle.[34] Previous studies in skin and cartilage tissues of Recql4-deficient mice and in human fibroblasts after *RECQL4* downregulation demonstrated exuberant senescence.[35-37] Cell cycle arrest in senescence is induced by activation of p53 and p21 and maintained by p16.[38]

To analyze if increased senescence could contribute to aging symptoms in CRIPT deficiency, we stained skin samples from *CRIPT* individual #1 and #2 and from 20- and 72-year-old healthy controls for p53, p16, and p21. The skin of the younger control was negative for senescence markers (Figure 3A). In contrast, keratinocytes in the skin of the *CRIPT* children #1 and #2 showed strong expression of p53. In the 2-year-old *CRIPT* individual #1, there was additionally strong expression of p21 and p16, similar to the older control. The activity of senescence-associated ß-galactosidase (SA-ß-galactosidase) in fibroblasts, a marker of senescent cells, was quantified by

FACS. The SA-ß-galactosidase activity was significantly higher in patient-derived CRIPT-deficient fibroblasts from individuals #1 and #2 compared with that of control (Figure 3C). The extent of senescence in cultured cells depends on the age and passage number and can be influenced by selective pressure. To better control these factors, we downregulated CRIPT expression by siRNA in wild-type fibroblasts (Figure 3D). CRIPT downregulation caused a significant 2.5-fold upregulation of SA-ß-galactosidase activity when compared with negative control siRNA (Figure 3E and F). In line with the increased senescence observed in RECQL4-deficient tissues, CRIPT deficiency also induces cellular senescence.

Karyotypes and mitotic progression are unchanged in patient-derived cells

The underlying mechanism driving cellular senescence in CRIPT- and RECQL4-deficient cells is unknown. Senescence can be induced by mitotic, genotoxic, or oxidative stress.

In up to 6% of RTS cases, low-level mosaicism of numerical or structural chromosomal aberrations, most frequently of chromosomes 8, 7, or 2, were observed in lymphocytes and fibroblasts, suggesting a defect in chromosomal segregation.[2,10,11] In addition, in cells derived from a viable mouse model of RTS, up to 25% of cells exhibited defective sister chromatid cohesion with precocious segregation of sister chromatids.[39] Karyotypes of lymphocytes (#1 and #2) and fibroblasts (#1) from *CRIPT* individuals did not indicate increased rates of chromosomal aberrations, precocious segregation of sister chromatids, or sister chromatid exchanges (>100 cells evaluated, Figure 4A and H; Supplemental Figure 3G). For the detection of low-grade mosaicism, interphase fluorescence in situ hybridization of chromosomes 2, 7, 8, 11, and 17 was performed but no isochromosomes were detected (Figure 4B). To search for somatic structural variants (SVs) and copy number variants, fibroblasts and lymphocytes of individual #1 were additionally analyzed with optical genome mapping (Bionano Genomics). Rare germline SVs present in both tissues with variant allele fractions were filtered out. Using stringent filter settings, we did not detect somatic SVs or copy number variants with variant allele fractions ranging from >5% to 10% (single-cell SVs cannot be excluded, Figure 4C).

RECQL4 is a microtubule-associated protein and localizes to the mitotic spindle.[18,39] RECQL4 downregulation in HeLa cells delayed mitotic progression and induced chromosome misalignment, but these aberrations were not observed in patient-derived RECQL4-deficient fibroblasts.[18] CRIPT also binds to microtubules and was recently suggested to be crucial for redox-dependent microtubule depolymerization at spindle ends during anaphase.[26,30] In this publication, it was shown that CRIPT knockout and cysteine substitution of CRIPT in HeLa cells caused either
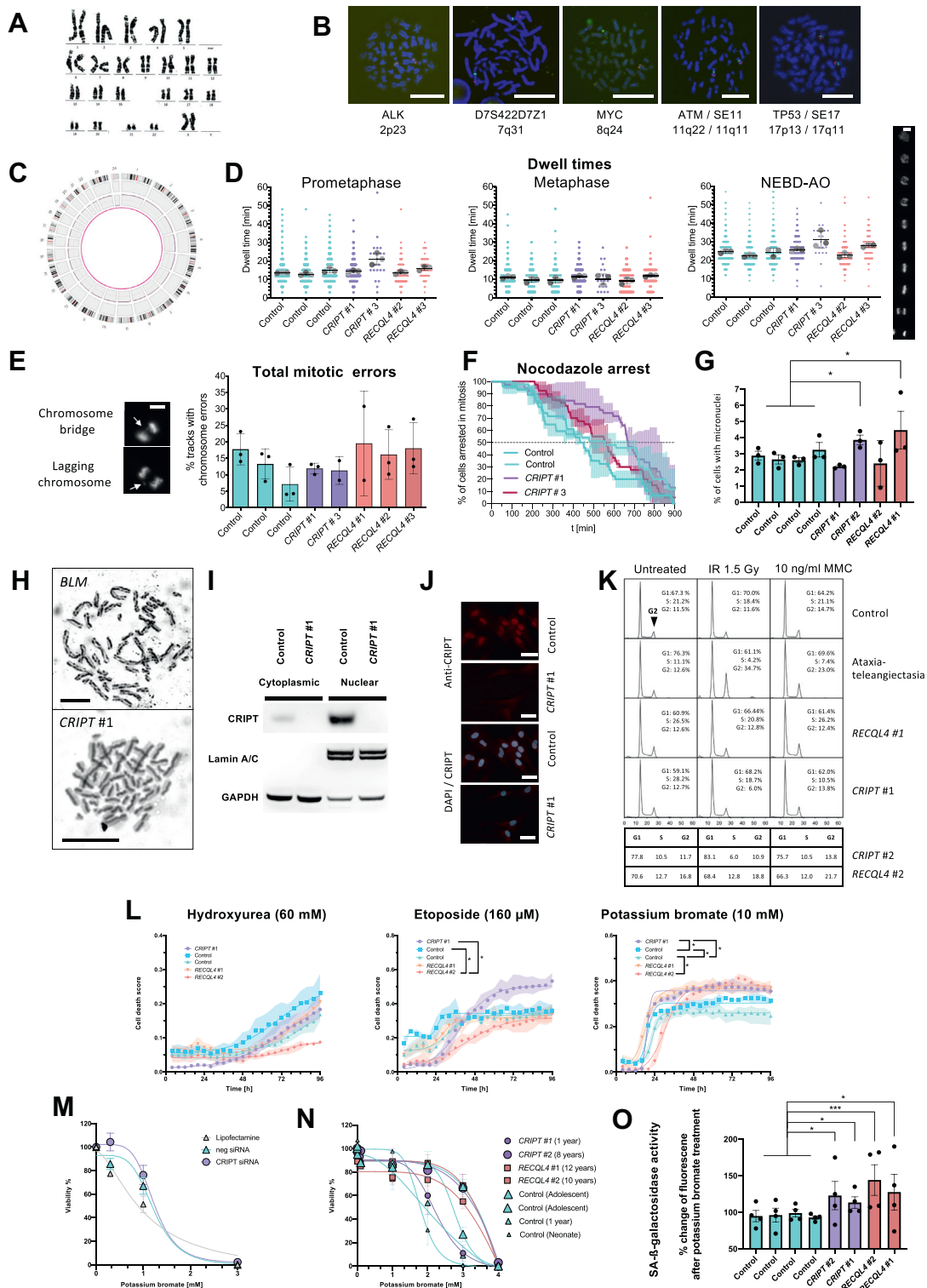
Figure 4 **Analysis of chromosomal aberrations, mitotic progression, mitotic errors and sensitivity to chemotoxic stress in CRIPT-and RECQL4-deficient cells.** A. Representative karyograms of cultured fibroblasts from *CRIPT* individual #1 showing no numerical or structural aberrations B. No mosaicism of numerical or structural aberrations detectable by inter- and metaphase-FISH (>1000 cells) using different probes. Representative metaphases are shown. C. Circos plot of somatic SVs and CNVs of *CRIPT* individual #1 analyzed by optical genome mapping (Bionano Genomics; minimal detectable variant allele fraction 5%-10%). After filtering rare SVs that were present in both tissues with variant allele fractions close to 50% to 100% (suggestive of germline SVs), no somatic SVs or CNVs were detected D. Mitotic progression was measured by live-cell imaging and quantified with the machine learning-algorithm CecogAnalyzer.[29] Superblots of mitotic timing of prometaphase, metaphase, and the time from NEBD to anaphase onset in cultured cells from healthy controls and from *CRIPT* and *RECQL4* individuals: The thick gray dots represent the means of the populations of each independent experiment. The colored small dots

mitotic arrest or multipolar spindles and/or chromosome alignment with long-lasting spindle remnants. To test if CRIPT patient–derived fibroblasts show a similar phenotype with mitotic arrest, we analyzed mitotic progression and mitotic errors in patient-derived CRIPT- and RECQL4-deficient cells by live-cell imaging. Interestingly, prometaphase to anaphase progression did not significantly differ between control and CRIPT- or RECQL4-deficient and control cells (Figure 4D, *P* values of one-way analysis of variance: Supplemental Table 6). In RECQL4- and CRIPT-deficient cells, incidence of lagging chromosomes, misaligned chromosomes, or chromosomal bridges was not consistently increased when compared with control cells (Figure 4E; Supplemental Figure 3B-D). In addition, the proportion of dividing cells with tilted spindle axes indicative of spindle microtubule defects was not different from that of controls (Supplemental Figure 3E).

Because a defective spindle assembly checkpoint (SAC) can cause low levels of chromosome segregation errors, we also intended to check the integrity of the SAC.[40] Challenging cells with nocodazole, a drug that disturbs the microtubule polymerization, results in prometaphase arrest via SAC activation. The duration of this arrest serves as a readout for SAC integrity. After nocodazole challenge, the duration of arrest was not reduced in CRIPT-deficient fibroblasts, indicating an intact SAC (Figure 4F).

Micronuclei can result from chromosome malsegregation, for example, arising from mitotic spindle or kinetochore defects, or from acentric chromosome fragments generated by unrepaired DNA breaks. In patient-derived RECQL4-deficient fibroblasts, an increased number of micronuclei was reported.[18] We quantified the number of micronuclei in *CRIPT* #1 and #2 and *RECQL4* #1 and #2 patient-derived fibroblasts and only found inconsistently increased numbers of micronuclei in fibroblasts from *CRIPT* #2 (3.8%) and *RECQL4* #1 (4.4%) when compared with that of control cells (2.8%) (Figure 4G). However, because of the high variability between cell lines, no clear conclusions can be drawn.

Nuclear localization of *CRIPT* and sensitivity to genotoxic stress

CRIPT was originally described as a cytoplasmic, microtubule-binding protein that localizes to synapses in neurons.[25,26] Recently, it was shown that during interphase CRIPT is localized in the nucleus.[30] By immunofluorescence and immunoblotting of cytoplasmic and nuclear fractions, we could confirm that CRIPT is expressed in both cytoplasmic and, more pronounced, in nuclear compartments in wild-type fibroblasts (Figure 4I and J).

Based on initial findings of RECQL4 localizing to nuclear foci, RECQL4 was suggested to be involved in DNA repair.[41] Later studies demonstrated that RECQL4 acts in DNA replication, homologous recombination, nonhomologous end joining, base excision repair, and telomere maintenance.[14-17] However, studies with primary cell lines derived from Recql4-deficient mice and RTS individuals yielded conflicting results regarding sensitivity to genotoxic agents. In fibroblasts from 10 RTS individuals, only agents interfering with DNA replication (eg, hydroxyurea) impaired growth in colony survival assays, whereas cells showed only minor sensitivity to DNA damaging agents (eg, cisplatin).[42]

We analyzed the sensitivity of patient-derived fibroblasts to ionizing radiation (IR; 1.5 Gy) and mitomycin C using a diagnostic pipeline for screening for ataxia-telangiectasia, ligase-IV-syndrome, and Fanconi anemia.[43,44] The sensitivity of fibroblasts from *CRIPT* #1 and #2 and *RECQL4* #1 and #2 to IR and mitomycin C was in the range of control cells, only showing a trend toward a higher shift from S to G1 phase after IR (Figure 4K). These findings are in line with the unremarkable sensitivity of Recql4 knockout mouse embryonic fibroblasts to IR.[45]

represent the time for each cell. No differences in dwell timing were observed. *P* values of ordinary one-way ANOVA are reported in Supplemental Table 6. E. Numbers of mitotic cell trajectories with chromosomal errors, including misaligned, lagging chromosomes, and chromosome bridges. Fisher's exact test was used to compare the pooled percentages and showed no differences between CRIPT-, RECQL4-deficient, and control cells. F. After nocodazole (100 ng/mL) treatment for 30 minutes, the arrest time of CRIPT-deficient fibroblasts is not reduced when compared with control cells. D-F show the results of 3 pooled experiments. Mean ± SD. G. The percentage of cells with micronuclei was inconsistently increased in fibroblasts from individuals CRIPT #2 and RECQL4 #1. H. Differential staining of sister chromatids in chromosomes from patient-derived lymphocytes (BS: Bloom Syndrome, CRIPT #1). The number of sister chromatid exchanges has been assessed by light microscopy. I. Western blot after extraction of cytoplasmic and nuclear (laminin A/C) fractions from fibroblasts. J. Immunofluorescent labeling of CRIPT (red) showing the presence of CRIPT in the cytoplasm and in the nucleus (DAPI, blue). K. Cell cycle distribution of primary fibroblasts (control, ataxia-telangiectasia, *RECQL4* #1 and #2, *CRIPT* #1 and #2) after ionizing radiation 1.5 Gy or exposure to mitomycin C (MMC). G2: G2/m phase of the cell cycle. L. IncuCyte live-cell imaging of cell viability of patient-derived fibroblasts upon challenge with hydroxyurea, etoposide, and potassium bromate. One-way-ANOVA, *P* < .05. M, N Cell viability of fibroblasts analyzed by CellTiterGlo Assay (Promega) (M) after siRNA targeting of CRIPT expression and (N) in patient-derived fibroblasts after potassium bromate challenge for 72 hours measured, means of relative change of viability of 3 independent experiments, O. Relative change of senescence-associated ß-galactosidase activity after treatment of patient-derived fibroblasts with low-dose potassium bromate (10 μM) for 5 days, quantified by flow cytometry. Mean ± SD. Scale bars = 10 μm. *ANOVA*, analysis of variance; *BLM*, BLM gene; *CNV*, copy number variant; *FISH*, fluorescence in situ hybridization; *MMC*, mitomycin C; *NEBD*, nuclear envelope breakdown; *neg siRNA*, negative control small interfering RNA; *SV*, structural variant; *RTS*, Rothmund-Thomson syndrome.

We next screened the sensitivity to hydroxyurea, etoposide, and potassium bromate by live-cell imaging of cell viability. Hydroxyurea interferes with DNA replication. In contrast to a previous report, RECQL4- and CRIPT-deficient fibroblasts did not show an increased susceptibility to hydroxyurea compared with those in controls (Figure 4L).[42] The topoisomerase II inhibitor etoposide induces double-strand breaks. Although fibroblasts from *CRIPT* individual #1 showed a slightly increased sensitivity to etoposide, the overall sensitivity was in the range of controls (Figure 4L). Potassium bromate oxidizes DNA generating 7,8-dihydro-8-oxoguanine; 7,8-dihydro-8-oxoguanine is repaired by base excision repair, and *RECQL4* knockout was reported to impair base excision repair.[46] The fibroblasts from individuals CRIPT #1 and RECQL4 #1 and #2 showed a mildly increased sensitivity to potassium bromate (10 mM) compared with control (Figure 4L). To further explore a potential sensitivity to potassium bromate, we downregulated CRIPT expression in wild-type fibroblasts. Although targeting CRIPT expression by siRNA caused a significant decrease in the number of proliferating cells, the sensitivity to potassium bromate, or alternatively oxidative stress by hydrogen peroxide, was unaffected by CRIPT downregulation (Figure 4M; Supplemental Figure 4). Likewise, patient-derived CRIPT- or RECQL4-deficient fibroblasts were not more sensitive to different doses of potassium bromate than controls. As expected, however, we noted a trend toward a higher sensitivity to potassium bromate in fibroblasts with shorter doubling times (Supplemental Figure 3A; Figure 4N). Because this was not systematically assessed, further studies would be required to prove this association. To investigate if sublethal doses of potassium bromate might trigger cellular senescence, we challenged patient-derived fibroblasts with a low concentration of potassium bromate (10 µM) for 5 days. Although the SA-ß-galactosidase activity remained unchanged in control fibroblasts, CRIPT- and RECQL4-deficient fibroblasts responded with mild upregulation of SA-ß-galactosidase activity upon low concentration potassium bromate challenge (Figure 4O).

In conclusion, though low-level genotoxic stress might induce cellular senescence in CRIPT- and RECQL4-deficient fibroblast, the overall sensitivity to lethal doses of genotoxic stress is in the range of control cells.

Discussion

RTS is characterized by poikiloderma, sparse hair, small stature, susceptibility to cancer, and cataracts, features usually found in the aging population. Genetically, RTS is a heterogeneous disease with *RECQL4* and *ANAPC1* as the established disease-causing genes. However, in up to 30% of RTS individuals, no causative variants are detected in either *RECQL4* or *ANAPC1,* suggesting other, not yet identified disease genes.

We initially report 2 individuals who fulfill the diagnostic RTS criteria and lack pathogenic variants in *RECQL4* or *ANAPC1,* but who both have biallelic variants in the *CRIPT* gene. Biallelic variants in *CRIPT* have been reported in 4 individuals in the literature, accounting for a multisystemic disorder, including short stature, skin rash, skeletal, and neurodevelopmental anomalies.[22-24] Our systematic evaluation of the clinical, histologic, and radiologic features showed that all 6 *CRIPT* individuals matched very well to the clinical spectrum of RTS. In a computational approach, facial images of *CRIPT* individuals showed the highest similarity to RTS individuals when compared with other premature aging and poikiloderma-associated syndromes. Given the phenotypic overlap, we propose that, in addition to *RECQL4* and *ANAPC1*, *CRIPT* causes an RTS-like syndrome.

One possible explanation why the published *CRIPT* cases had not yet been linked to RTS is that most ectodermal features in RTS develop over time starting at the age of 3 to 6 months and that published *CRIPT* individuals had not yet manifested the full dermatologic picture, as exemplified by follow-up data on individuals #3 and #5 (Figure 1D and E).[22,23]

All *CRIPT* individuals presented with mild motor and more severe speech developmental delay, 5 of 6 *CRIPT* individuals had microcephaly proportional to body size, and 4 of 6 had well-controlled or refractory epilepsy. Although cognition has not formally been assessed in RTS, *RECQL4* individuals from the RTS registry are reported to have mild speech delay and minor delays in meeting developmental milestones.[13] In addition, cases of non-*RECQL4*-RTS individuals with more profound neurodevelopmental delay have been reported.[5-9] Mechanistically, the neurodevelopmental phenotype of CRIPT deficiency might be related to the known function of CRIPT in dendritic and synaptic plasticity and memory formation.[30,45]

POIKTM and poikiloderma with neutropenia (PN) are 2 poikiloderma syndromes that have been published as distinct diseases. Although the facial profiles of POIKTM and PN overlap with RTS, these 2 diseases have features (PN: no sparse hair and no skeletal defect; POIKTMP: psoriasis-like lesions, blisters, almost obligatory internal organ involvement, myopathy, and contractures) that clearly distinguish them from RTS. In view of the neurodevelopmental phenotype as apparently outstanding feature of *CRIPT* individuals, it is debatable if the *CRIPT*-associated RTS-like syndrome should rather be classified as a distinct RTS-like disease entity or as a novel subtype of RTS (eg, type 3). Cataracts and the absence of cancer are the typical features of RTS type 1. Additionally, developmental delay has been observed in 2 of 10 *ANAPC1* RTS type 1 individuals.[30,46] *CRIPT* individual #2 developed bilateral cataracts at the age of 8 years; none of the *CRIPT* individuals had cancer to date and all have developmental delay. In view of this overlap, the clinical phenotype of *CRIPT* deficiency appears to be closer to RTS type 1 than 2. However, long-time clinical follow-up is warranted to

systematically assess the risk of cancer and cataracts and neurologic development and to compare the frequency of these features in *CRIPT*, *ANAPC1*, and *RECQL4* individuals.

Although CRIPT was primarily studied in the context of neuronal connectivity and recently mitotic spindle disassembly, RECQL4 has been implicated in many cellular processes, including DNA repair, cellular senescence, and cell cycle progression, but the crucial mechanism that accounts for the multisystemic and aging-related findings in RTS is under debate.[30,47] The so far unrecognized link between *CRIPT* and RTS opens avenues to delineate further the molecular pathology of RTS symptoms. In the experimental part of this study, we searched for shared cellular pathways of CRIPT- and RECQL4-deficient cells, focusing on cellular senescence, mitotic progression, and sensitivity to genotoxic stress.

Similar to RECQL4 deficiency, we found that CRIPT deficiency induces a senescence phenotype as demonstrated by high levels of p16, p21, and p53 expression in skin biopsies and increased SA-ß-galactosidase activity in patient-derived fibroblasts and upon CRIPT downregulation. Senescent cells change their metabolic profile into proinflammatory secretory cells and this senescence-associated secretory inflammatory phenotype might explain the immune cell infiltration and dilated blood vessels observed in skin from *CRIPT* individuals and other poikiloderma disorders.[48] Overriding senescence of dermal hair matrix or papilla cells might cause a loss of the hair cuticle cells that we observed by electron microscopy in *CRIPT* and *RECQL4* individuals.

Senescence can occur in response to different kinds of stress, including genotoxic and oxidative damage and mitotic errors. Although structural and numerical chromosomal aberrations were reported in subsets of RTS individuals (eg, in 3 of 17 published individuals), we did not detect any chromosomal aberrations in *CRIPT* patient–derived cells.[2] Fibroblasts from *RECQL4* or *CRIPT* individuals progressed normally through mitosis, and the mitotic defects were not overrepresented compared with those from controls. In summary, in patient-derived cells with disease-associated *RECQL4* and *CRIPT* variants, there were no quantifiable mitotic defects. In a previous study, the number of misaligned chromosomes increased after RECQL4 downregulation in HeLa cells, but it was normal in *RECQL4* patient–derived cells.[18] Similarly, the divergent results for CRIPT with regard to mitotic defects might be likely because of differences between patient-derived fibroblasts and immortalized cells, for example, cancer cells but do not exclude a functional role of CRIPT or RECQL4 in mitosis.

Cellular senescence could also be triggered by DNA repair defects and genomic instability. The overall sensitivity of *RECQL4* and *CRIPT* patient–derived cells and fibroblasts after siRNA downregulation of CRIPT expression to different types of genotoxic stress was in the range of control cells.

In conclusion, we identified *CRIPT* as a novel RTS-like syndrome causing gene with neurologic impairment and further expand the genetic heterogeneity of the RTS spectrum of disorders. We searched for shared cellular defects as the drivers for overlapping RTS phenotypes and narrowed down that CRIPT and RECQL4 deficiency are both associated with (1) increased cellular senescence and (2) only mild sensitivity to chemotoxic agents, (3) while the numbers of mitotic errors was not significantly different from controls. Of note, only CRIPT- and RECQL4-deficient patient-derived fibroblasts were available for this study, and future studies elucidating the functional impact in APC1-deficient cells are warranted. Thus, the question regarding which precise mechanism drives senescence remains unanswered at the current stage.

Our findings will open the door for further studies exploring the role of *CRIPT*, *RECQL4*, and also *ANAPC1* in preventing cellular senescence and the potential of senolytic drugs as a therapeutic approach. "Splitter and lumper debates" are decisive in the field of syndromic diseases. Formal neurologic assessment of RTS individuals and long-term clinical follow-up of additional *CRIPT* individuals will add clarification to the debate whether the *CRIPT*-associated RTS-like syndrome should rather be split as a separate disease entity or rather should be classified as a novel subtype of RTS.

Data Availability

Data and materials that are not provided in this article because of space limitations will be supplied upon request for purposes of replicating procedures and results and follow-up research studies. Please send your request to luisa.aver@gmail.com or felix.distelmaier@med.uni-duesseldorf.de.

Acknowledgments

Funding

Author Information

Conceptualization: L.A., F.D.; Data Curation (clinical data): L.A., S.M., E.A.F., S.L., P.B., J.A.O.; Formal Analysis (clinical data): L.A., S.M., E.A.F., S.L., T.D., T.-C.H., J.A.O., T.B., J.S., D.W., L.L.W., F.D.; Funding Acquisition: P.K., E.M., W.A., R.D.J., V.v.F., F.D.; Investigation (functional data): L.A., M.A.H., D.M.-A., A.S., K.N., A.H., P.B., B.H., W.A., R.D.J., V.v.F., M.S., E.G., L.L., W.J., D.S., R.K.; Methodology: L.A., D.M.-A., T.-C.H., K.N., P.B., P.K., W.A., R.D.J., D.S., R.K., F.D.; Project Administration: L.A., F.D.; Resources: P.K., E.M., W.A., R.D.J., V.v.F., F.D.; Software: D.M.-A., A.H., N.F., P.K., R.D.J.; Supervision: W.A., R.D.J., L.L.W., F.D.; Validation: L.L.W., F.D.; Visualization: L.A., M.A.H., D.M.-A., T.-C.H., A.S., B.H., N.F., V.v.F.; Writing-original draft: L.A., M.A.H.; Writing-review and editing: L.A., D.M.-A., T.B., J.S., T.D., L.L.W., W.A., E.M., D.S., D.W., F.D.

Ethics Declaration

The study was performed according to the Declaration of Helsinki and was approved by the institutional ethical review board (Heinrich-Heine-University, Düsseldorf, vote 2021-1340-LA/FD). The legal guardians provided written informed consent to participate in the study and gave their explicit permission for the publication of photographs. The authors attest that the research included in this report was conducted in a manner consistent with the principles of research ethics, such as those described in the Declaration of Helsinki and/or the Belmont Report. In particular, this research was conducted with the voluntary, informed consent of any research participants, free of coercion or coercive circumstances, and received institutional review board or research ethics committee approval consistent with the principles of research ethics and the legal requirements of the lead authors' jurisdiction(s).

Conflict of Interest

The authors declare no conflicts of interest.

Additional Information

The online version of this article (https://doi.org/10.1016/j.gim.2023.100836) contains supplementary material, which is available to authorized users.

Authors

Luisa Averdunk[1,*] iD, Maxim A. Huetzen[2,3,4,5], Daniel Moreno-Andrés[6], Reinhard Kalb[7], Shane McKee[8], Tzung-Chien Hsieh[9], Annette Seibt[1], Marten Schouwink[1], Seema Lalani[10], Eissa Ali Faqeih[11], Theresa Brunet[12,13], Peter Boor[14], Kornelia Neveling[15], Alexander Hoischen[15], Barbara Hildebrandt[16], Elisabeth Graf[12], Linchao Lu[17], Weidong Jin[17], Joerg Schaper[18], Jamal A. Omer[19], Tanguy Demaret[20], Nicole Fleischer[21], Detlev Schindler[7], Peter Krawitz[9], Ertan Mayatepek[1], Dagmar Wieczorek[16], Lisa L. Wang[17], Wolfram Antonin[6], Ron D. Jachimowicz[2,3,4,5], Verena von Felbert[22], Felix Distelmaier[1,*]

Affiliations

[1]Department of General Pediatrics, Neonatology and Pediatric Cardiology, Medical Faculty, University Hospital Düsseldorf, Heinrich-Heine-University, Düsseldorf, Germany; [2]Max Planck Research Group Mechanisms of DNA Repair, Max Planck Institute for Biology of Ageing, Cologne, Germany; [3]Department I of Internal Medicine, Center for Integrated Oncology Aachen Bonn Cologne and Duesseldorf, Faculty of Medicine and University Hospital Cologne, University of Cologne, Cologne, Germany; [4]Cologne Excellence Cluster on Cellular Stress Response in Aging-Associated Diseases, University of Cologne, Cologne, Germany; [5]Center for Molecular Medicine Cologne, University of Cologne, Cologne, Germany; [6]Institute of Biochemistry and Molecular Cell Biology, Medical School, RWTH Aachen University, Aachen, Germany; [7]Institute for Human Genetics, Biocenter, University of Würzburg, Würzburg, Germany; [8]Northern Ireland Regional Genetics Service, Belfast City Hospital, Belfast HSC Trust, Belfast, United Kingdom; [9]Institute of Genomic Statistics and Bioinformatics, University of Bonn, Bonn, Germany; [10]Department of Molecular Genetics, Baylor College of Medicine, Houston, TX; [11]Division of Medical Genetics, Children's Specialized Hospital, King Fahad Medical City, Riyadh, Saudi Arabia; [12]Technical University of Munich,

School of Medicine, Institute of Human Genetics, Munich, Germany; [13]Institute of Neurogenomics, Helmholtz Zentrum München, Munich, Germany; [14]Institute of Pathology and Electron Microscopy Facility, Medical Faculty, RWTH Aachen University, Aachen, Germany; [15]Department of Human Genetics, Radboud University Medical Center, Nijmegen, The Netherlands; [16]Institute of Human Genetics, University Hospital Düsseldorf, Heinrich-Heine-Universität, Düsseldorf, Germany; [17]Division of Hematology/Oncology, Department of Pediatrics, Texas Children's Cancer Center, Baylor College of Medicine, Houston, TX; [18]Center of Rare Diseases, Medical Faculty, Heinrich-Heine-University, Düsseldorf, Germany; [19]Department of General Pediatrics, Children's Specialized Hospital, King Fahad Medical City, Riyadh, Saudi Arabia; [20]Centre de Génétique Humaine, Institut de Pathologie et Génétique, Gosselies, Belgium; [21]FDNA Inc., Boston, MA; [22]Department of Dermatology and Allergology, Medical Faculty, RWTH Aachen University, Aachen, Germany

References

1. Vennos EM, Collins M, James WD. Rothmund-Thomson syndrome: review of the world literature. *J Am Acad Dermatol.* 1992;27(5Pt1):750-762. http://doi.org/10.1016/0190-9622(92)70249-f

2. Wang LL, Levy ML, Lewis RA, et al. Clinical manifestations in a cohort of 41 Rothmund-Thomson syndrome patients. *Am J Med Genet.* 2001;102(1):11-17. http://doi.org/10.1002/1096-8628(20010722)102:1<11::aid-ajmg1413>3.0.co;2-a

3. Rothmund A. Ueber Cataracten in Verbindung mit einer eigenthümlichen Hautdegeneration. *Graefes Archiv für Ophthalmologie.* 1868;14(1):159-182. http://doi.org/10.1007/BF02720945

4. Thomson MS. An hitherto undescribed familial disease. *Br J Dermatol.* 1923;35(12):455-462. http://doi.org/10.1111/j.1365-2133.1923.tb09077.x

5. Gelaw B, Ali S, Becker J. Rothmund-Thomson syndrome, Klippel-Feil syndrome, and osteosarcoma. *Skeletal Radiol.* 2004;33(10):613-615. http://doi.org/10.1007/s00256-004-0798-2

6. Hall JG, Pagon RA, Wilson KM. Rothmund-Thomson syndrome with severe dwarfism. *Am J Dis Child.* 1980;134(2):165-169. http://doi.org/10.1001/archpedi.1980.02130140039013

7. Kassner EG, Qazi QH, Haller JO. Rothmund-Thomson syndrome (poikiloderma congenitale) associated with mental retardation, growth disturbance, and skeletal features. *Skeletal Radiol.* 1977;2(2):99-103. http://doi.org/10.1007/BF00360989

8. Kraus BS, Gottlieb MA, Meliton HR. The dentition in Rothmund's syndrome. *J Am Dent Assoc.* 1970;81(4):895-915. http://doi.org/10.14219/jada.archive.1970.0328

9. Nathanson M, Dandine M, Gaudelus J, Mousset S, Lasry D, Perelman R. Rothmund-Thompson syndrome with glaucoma. Endocrine study. *Sem Hop.* 1983;59(48):3379-3384.

10. Miozzo M, Castorina P, Riva P, et al. Chromosomal instability in fibroblasts and mesenchymal tumors from 2 sibs with Rothmund-Thomson syndrome. *Int J Cancer.* 1998;77(4):504-510. http://doi.org/10.1002/(sici)1097-0215(19980812)77:4<504::aid-ijc5>3.0.co;2-y

11. Lindor NM, Devries EMG, Michels VV, et al. Rothmund-Thomson syndrome in siblings: evidence for acquired in vivo mosaicism. *Clin Genet.* 1996;49(3):124-129. http://doi.org/10.1111/j.1399-0004.1996.tb03270.x

12. Kitao S, Shimamoto A, Goto M, et al. Mutations in RECQL4 cause a subset of cases of Rothmund-Thomson syndrome. *Nat Genet.* 1999;22(1):82-84. http://doi.org/10.1038/8788

13. Ajeawung NF, Nguyen TTM, Lu L, et al. Mutations in ANAPC1, encoding a scaffold subunit of the anaphase-promoting complex, cause Rothmund-Thomson syndrome type 1. *Am J Hum Genet.* 2019; 105(3):625-630. http://doi.org/10.1016/j.ajhg.2019.06.011

14. Sangrithi MN, Bernal JA, Madine M, et al. Initiation of DNA replication requires the RECQL4 protein mutated in Rothmund-Thomson syndrome. *Cell.* 2005;121(6):887-898. http://doi.org/10.1016/j.cell.2005.05.015

15. Kumata Y, Tada S, Yamanada Y, et al. Possible involvement of RecQL4 in the repair of double-strand DNA breaks in Xenopus egg extracts. *Biochim Biophys Acta.* 2007;1773(4):556-564. http://doi.org/10.1016/j.bbamcr.2007.01.005

16. Lu H, Shamanna RA, Keijzers G, et al. RECQL4 promotes DNA end resection in repair of DNA double-strand breaks. *Cell Rep.* 2016;16(1):161-173. http://doi.org/10.1016/j.celrep.2016.05.079

17. Ghosh AK, Rossi ML, Singh DK, et al. RECQL4, the protein mutated in Rothmund-Thomson syndrome, functions in telomere maintenance. *J Biol Chem.* 2012;287(1):196-209. http://doi.org/10.1074/jbc.M111.295063

18. Yokoyama H, Moreno-Andres D, Astrinidis SA, et al. Chromosome alignment maintenance requires the MAP RECQL4, mutated in the Rothmund-Thomson syndrome. *Life Sci Alliance.* 2019;2(1): e201800120. http://doi.org/10.26508/lsa.201800120

19. Xu X, Liu Y. Dual DNA unwinding activities of the Rothmund-Thomson syndrome protein, RECQ4. *EMBO J.* 2009;28(5):568-577. http://doi.org/10.1038/emboj.2009.13

20. Shirayama M, Tóth A, Gálová M, Nasmyth K. APC(Cdc20) promotes exit from mitosis by destroying the anaphase inhibitor Pds1 and cyclin Clb5. *Nature.* 1999;402(6758):203-207. http://doi.org/10.1038/46080

21. Larizza L, Roversi G, Volpi L. Rothmund-Thomson syndrome. *Orphanet J Rare Dis.* 2010;5:2. http://doi.org/10.1186/1750-1172-5-2

22. Leduc MS, Niu Z, Bi W, et al. CRIPT exonic deletion and a novel missense mutation in a female with short stature, dysmorphic features, microcephaly, and pigmentary abnormalities. *Am J Med Genet A.* 2016;170(8):2206-2211. http://doi.org/10.1002/ajmg.a.37780

23. Shaheen R, Faqeih E, Ansari S, et al. Genomic analysis of primordial dwarfism reveals novel disease genes. *Genome Res.* 2014;24(2):291-299. http://doi.org/10.1101/gr.160572.113

24. Akalın A, Şimşek-Kiper PÖ, Taşkıran EZ, Karaosmanoğlu B, Utine GE, Boduroğlu K. A novel biallelic CRIPT variant in a patient with short stature, microcephaly, and distinctive facial features. *Am J Med Genet A.* 2023;191(4):1119-1127. http://doi.org/10.1002/ajmg.a.63120

25. Niethammer M, Valtschanoff JG, Kapoor TM, et al. CRIPT, a novel postsynaptic protein that binds to the third PDZ domain of PSD-95/SAP90. *Neuron.* 1998;20(4):693-707. http://doi.org/10.1016/s0896-6273(00)81009-0

26. Passafaro M, Sala C, Niethammer M, Sheng M. Microtubule binding by CRIPT and its potential role in the synaptic clustering of PSD-95. *Nat Neurosci.* 1999;2(12):1063-1069. http://doi.org/10.1038/15990

27. Hsieh TC, Bar-Haim A, Moosa S, et al. GestaltMatcher facilitates rare disease matching using facial phenotype descriptors. *Nat Genet.* 2022;54(3):349-357. http://doi.org/10.1038/s41588-021-01010-x

28. Villegas J, McPhaul M. Establishment and culture of human skin fibroblasts. *Curr Protoc Mol Biol.* 2005;Chapter (28):Unit 28.3. https://doi.org/10.1002/0471142727.mb2803s71

29. Held M, Schmitz MHA, Fischer B, et al. CellCognition: time-resolved phenotype annotation in high-throughput live cell imaging. *Nat Methods.* 2010;7(9):747-754. http://doi.org/10.1038/nmeth.1486

30. Xu K, Wang C, Keinänen K, Li H, Cai C. Mitotic spindle disassembly in human cells relies on CRIPT having hierarchical redox signals. *J Cell Sci.* 2022;135(18):jcs259657. http://doi.org/10.1242/jcs.259657

31. Mehollin-Ray AR, Kozinetz CA, Schlesinger AE, Guillerman RP, Wang LL. Radiographic abnormalities in Rothmund-Thomson syndrome and genotype–phenotype correlation with RECQL4 mutation status. *AJR Am J Roentgenol.* 2008;191(2):W62-W66. http://doi.org/10.2214/AJR.07.3619

32. Kubota M, Yasunaga M, Hashimoto H, et al. IgG4 deficiency with Rothmund-Thomson syndrome: a case report. *Eur J Pediatr*. 1993; 152(5):406-408. http://doi.org/10.1007/BF01955898

33. Gurovich Y, Hanani Y, Bar O, et al. Identifying facial phenotypes of genetic disorders using deep learning. *Nat Med*. 2019;25(1):60-64. http://doi.org/10.1038/s41591-018-0279-0

34. Lombard DB, Chua KF, Mostoslavsky R, Franco S, Gostissa M, Alt FW. DNA repair, genome stability, and aging. *Cell*. 2005;120(4):497-512. http://doi.org/10.1016/j.cell.2005.01.028

35. Lu H, Fang EF, Sykora P, et al. Senescence induced by RECQL4 dysfunction contributes to Rothmund-Thomson syndrome features in mice. *Cell Death Dis*. 2014;5(5):e1226. http://doi.org/10.1038/cddis. 2014.168

36. Lu L, Harutyunyan K, Jin W, et al. RECQL4 regulates p53 function in vivo during skeletogenesis. *J Bone Miner Res*. 2015;30(6):1077-1089. http://doi.org/10.1002/jbmr.2436

37. Davis T, Tivey HSE, Brook AJC, Grimstead JW, Rokicki MJ, Kipling D. Activation of p38 MAP kinase and stress signalling in fibroblasts from the progeroid Rothmund-Thomson syndrome. *Age (Dordr)*. 2013;35(5):1767-1783. http://doi.org/10.1007/s11357-012-9476-9

38. Stein GH, Drullinger LF, Soulard A, Dulić V. Differential roles for cyclin-dependent kinase inhibitors p21 and p16 in the mechanisms of senescence and differentiation in human fibroblasts. *Mol Cell Biol*. 1999;19(3):2109-2117. http://doi.org/10.1128/MCB.19. 3.2109

39. Mann MB, Hodges CA, Barnes E, Vogel H, Hassold TJ, Luo G. Defective sister-chromatid cohesion, aneuploidy and cancer predisposition in a mouse model of type II Rothmund-Thomson syndrome. *Hum Mol Genet*. 2005;14(6):813-825. http://doi.org/10.1093/hmg/ddi075

40. Weaver BAA, Cleveland DW. Decoding the links between mitosis, cancer, and chemotherapy: the mitotic checkpoint, adaptation, and cell death. *Cancer Cell*. 2005;8(1):7-12. http://doi.org/10.1016/j.ccr.2005. 06.011

41. Petkovic M, Dietschy T, Freire R, Jiao R, Stagljar I. The human Rothmund-Thomson syndrome gene product, RECQL4, localizes to distinct nuclear foci that coincide with proteins involved in the maintenance of genome stability. *J Cell Sci*. 2005;118(18):4261-4269. http://doi.org/10.1242/jcs.02556

42. Jin W, Liu H, Zhang Y, Otta SK, Plon SE, Wang LL. Sensitivity of RECQL4-deficient fibroblasts from Rothmund-Thomson syndrome patients to genotoxic agents. *Hum Genet*. 2008;123(6):643-653. http://doi.org/10.1007/s00439-008-0518-4

43. Schindler D, Friedl R, Gavvovidis I, et al. Applications of cell cycle testing in fanconi anemia. In: *Fanconi Anemia*. Karger; 2007:110-130. http://doi.org/10.1159/000102552

44. Beamish H, Lavin MF. Radiosensitivity in Ataxia-telangiectasia: anomalies in radiation-induced cell cycle delay. *Int J Radiat Biol*. 1994;65(2):175-184. http://doi.org/10.1080/09553009414550211

45. Hoki Y, Araki R, Fujimori A, et al. Growth retardation and skin abnormalities of the Recql4-deficient mouse. *Hum Mol Genet*. 2003;12(18):2293-2299. http://doi.org/10.1093/hmg/ddg254

46. Duan S, Han X, Akbari M, Croteau DL, Rasmussen LJ, Bohr VA. Interaction between RECQL4 and OGG1 promotes repair of oxidative base lesion 8-oxoG and is regulated by SIRT1 deacetylase. *Nucleic Acids Res*. 2020;48(12):6530-6546. http://doi.org/10.1093/nar/gkaa392

47. Lu L, Jin W, Wang LL. Aging in Rothmund-Thomson syndrome and related RECQL4 genetic disorders. *Ageing Res Rev*. 2017;33:30-35. http://doi.org/10.1016/j.arr.2016.06.002

48. Young ARJ, Narita M. SASP reflects senescence. *EMBO Rep*. 2009;10(3):228-230. http://doi.org/10.1038/embor.2009.22